Orchid Academia Siraha
Vol. 3, Issue 1, Dec. 2024

ISSN: 2976-1379 (Print)
ISSN: 2976-1387 (Online)

First Principles Investigation of Structural, Electronic and Mechanical Properties of $NaVF_3$

Kshitiz Kshetri[1], Uchit Chaudhary[1*], Ependra Tamang[1,2], Gopi Chandra Kaphle[1,2*]

[1]Central Department of Physics, Tribhuvan University

[2]Department of Science, Sukuna Multiple Campus

[*]**Corresponding Authors:** gck223@gmail.com, gopi.kaphle@cdp.tu.edu.np, uchitchaudhary99@gmail.com

https://doi.org/10.3126/oas.v3i1.78150

Abstract

In this research, first principles calculations of NaVF3 perovskite are performed using the Quantum ESPRESSO software package. The structural, electronic, magnetic, and mechanical properties of $NaVF_3$ are computed. The electronic structure reveals that it exhibits half-metallic ferromagnetism, with conducting nature in the spin-up channel and non-conducting in the spin-down channel. The half-metallicity and ferromagnetism in $NaVF_3$ are further confirmed by the integral magnetic moment of 3 μ_B. The mechanical properties analysis reveals that $NaVF_3$ is mechanically stable, ductile, and displays significant elastic anisotropy.

Keywords: Quantum ESPRESSO, perovskite, half metallicity, ferromagnetism, anisotropy

Introduction

Fluoro perovskites belong to the family of perovskite structures, which are known for their unique properties. These structures have the formula ABX_3, where A and B are cations and X is an anion (Brittman et al., 2015). Fluoro perovskites are well known for their wide range of functional properties, including optoelectronics, thermoelectric, optical lithography, photovoltaics, and semiconductive applications (Erum & Iqbal, 2017; Khattak et al., 2023; Rahman et al., 2021; Rahman et al., 2023). Normally, fluoro perovskites have wide or ultrawide band gaps (Meziani et al., 2011; Neupane & Thapa, 2017; Pilania & Sharma, 2013; Sandeep et al., 2017; Shahzad et al., 2024; Rehman et al., 2021), making them suitable for lenses, ferroelectric, antiferromagnetic systems and optical technologies such as transparent and optical coatings (Gillani et al., 2021). In addition to the wide band gap, many fluoro perovskites also seem to exhibit half metallic ferromagnetism (Abdullah, Khan et al., 2022; Abdullah, Sajjad et al., 2022; Hashmi et al., 2016; Mubarak & Al-Omari, 2015). They show 100% spin-polarization at the fermi level. Such half metallic perovskites are considered to be suitable for spintronic applications and various fields of modern technology (Algahtani et al., 2023; Hamlat et al., 2020).

Inspired by its broader applications, Chenine et al. (2017) performed an investigation of the structural, electronic, magnetic, mechanical, and thermoelectric

 ISSN: 2976-1379 (Print)
ISSN: 2976-1387 (Online)

properties of fluoroperovskite NaVF3 within the framework of WIEN2k. They used PBE and TB-mBJ functionals in their calculations and found that NaVF3 is half-metallic and ferromagnetic in nature. Similarly, Rashid (2019) performed the first principles calculation of the structural, electronic, magnetic, optical, and thermoelectric properties of $NaVF_3$. He used PBEsol-GGA and mBJ functionals and found that $NaVF_3$ exhibits a semiconducting nature.

Driven by discrepancies in the two previous studies of $NaVF_3$, we intended to investigate the actual behaviors of $NaVF_3$ and for that purpose, we performed the calculations of the structural, electronic, magnetic and mechanical properties of $NaVF_3$ with a different approach and presented the results in this paper.

Computational Details

The computations in this work were performed on the foundation of density functional theory (DFT) (Hohenberg & Kohn, 1964; Kohn & Sham, 1965). The Materials Project database was used as the source of crystal structure information and basic data for calculations (Jain et al., 2013). The Quantum ESPRESSO software package (Giannozzi, Baroni et al., 2009; Giannozzi, Andreussi et al., 2017) was used for DFT calculations. The PBE and PBEsol variations of the Generalized Gradient Approximation (GGA) (Perdew, Burke et al., 1996; Perdew, Chevary et al., 1992; Perdew, Ruzsinszky et al., 2008) were used as exchange-correlation functionals to investigate structural, electronic, magnetic, and mechanical properties. The sampling of the Brillouin zone was done through a Monkhorst-Pack (Monkhorst & Pack, 1976), 11 x 11 x 11 k-points mesh, and the cut-off energy was set to 100 Rydbergs. An extension to the quantum ESPRESSO, thermo_pw (Motornyi et al., 2018), was implemented for the approximation of mechanical properties.

Results and Discussion

Structural properties

$NaVF_3$ has a cubic unit cell and lies in the Pm-3m space group. The crystal structure of a unit cell of $NaVF_3$ is presented in Figure 1. The position of Na in $NaVF_3$ is at (0.0, 0.0, 0.0); similarly, V is located at (0.5, 0.5, 0.5); and three F atoms are at positions (0.0, 0.5, 0.5), (0.5, 0.0, 0.5), and (0.5, 0.5, 0.0), respectively. The cubic $NaVF_3$ structure was optimized using PBE and PBEsol in its ferromagnetic and non-magnetic states and the energy difference, $\triangle E = E_{FM} - E_{NM}$, was found to be negative, indicating higher stability of the ferromagnetic state. Taking it into account, further calculations of $NaVF_3$ in this paper were performed solely for the ferromagnetic state. The optimized lattice parameters were obtained as 4.12 $Å$ and 4.05 $Å$ for PBE and PBEsol, respectively, which are in good agreement with the experimental value of 3.94 $Å$ achieved by Shafer (1969). The formation and cohesive energy were calculated to show the chemical stability of the compound. The formation and cohesive energy of $NaVF_3$ can be expressed as (Ray et al., 2024).

$$E_{for} = E_{NaVF_3}^{total} - (E_{Na}^{bulk} + E_{v}^{bulk} + 3E_{F}^{bulk})$$

$$E_{coh} = E_{NaVF_3}^{total} - (E_{Na}^{iso} + E_{V}^{iso} + 3E_{F}^{iso})$$

Here, E_{for} and E_{coh} represent formation and cohesive energies for $NaVF_3$ while E^{bulk} and E^{iso} represent respective total energy per atom of Na, V and F atoms in bulk form and single isolated atom. The formation energy of $NaVF_3$ as calculated by using PBE functional was found to be -3.3407 eV/atom and the cohesive energy was found to be 4.6381 eV/atom. The negative value of formation energy points out that this compound is thermodynamically stable. Similarly, the equilibrium energies for different values of the lattice parameters were calculated, and the results were fitted to Birch-Murnaghan's equation of state (Murghan, 1944). From the Birch-Murnaghan fit, the bulk modulus, its first derivative, and the equilibrium lattice parameter of $NaVF_3$ are summarized in Table 1.

Figure 1 *Crystal Structure of NaVF3*

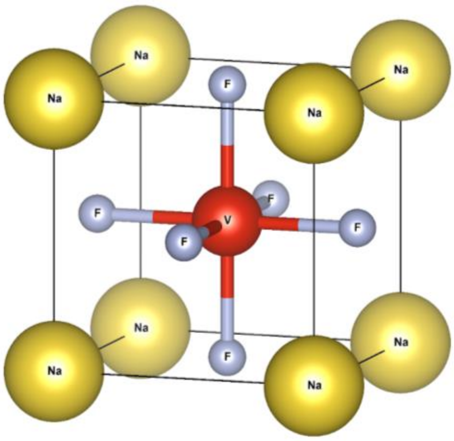

Table 1 *The Calculated Bulk Modulus (B), First Derivative of the Bulk Modulus (B'), Equilibrium Lattice Parameter (a_o), Formation Energy (E_{for}), and Cohesive Energy (E_{coh}) of $NaVF_3$*

Mode of calculation	B (GPa)	B'	a_o (Å)	E_{for} (eV/atom)	E_{coh} (eV/atom)
PBE	69.8	4.55	4.12	-3.3407	4.6381
PBEsol	78.1	4.65	4.05		
Other calculations	94.61[b], 98.03[c]	4.92[b]	4.04[b], 4.07[c], 3.94[a]		

[a]Experimental (shafer, 1969); [b]Theoretical (Chenine et al., 2017); [c]Theoretical (Rashid, 2019)

 ISSN: 2976-1379 (Print)
ISSN: 2976-1387 (Online)

Electronic Properties

Figures 2 and 3 demonstrate the band diagrams of $NaVF_3$ computed along the high symmetry points. The band diagrams indicate a half metallic nature of $NaVF_3$ with a conducting spin up channel and a non-conducting spin down channel with a clear band gap. Thus, the values of band gaps presented in this paper refer to the band gap from the spin down channel. The measured band gaps from PBE and PBEsol are 5.7436 eV and 5.9325 eV, respectively. Our findings revealed that $NaVF_3$ exhibits half-metallic behavior with a wide band gap in the spin-down channel, thereby supporting the conclusions drawn by Chenine et al. (2017). The previous study by Rashid (2019) illustrated it as a semiconductor. The discrepancies in the electronic structures are due to the use of different exchange-correlation functionals and the inherent limitations of computational methods. This highlights the importance of accurate approaches to obtain a more consistent and reliable interpretation of the material's electronic structure. The calculated values of the band gap lie in the ultraviolet range, which favours the substance for optoelectronic applications (Babu et al., 2020).

Further, to understand the atomic contributions to the electronic structure, we calculated the total and partial densities of states using both PBE and PBEsol functionals, as shown in Figures 4 and 5, respectively. The figures reveal that the total density of states intersects the Fermi level in the spin-up channel, thus indicating metallic behavior. However, the analysis displays a band gap in the spin-down channel for both approximations. Thus, the material shows 100% spin-polarized behavior at the Fermi level, which confirms its half-metallic ferromagnetic nature. According to the partial density of states, the d-orbital of V atom provide the most significant contribution to both valence and conduction bands, while Na and F atoms show a very small contribution.

Total and individual atomic magnetic moments also have been computed through calculations to analyze the magnetic characteristics of the system, as shown in Table 2. The magnetic properties of any compound require an integer magnetic moment value to exhibit half-metallic behavior, according to Attema et al. (2005). The obtained total integral magnetic moment of 3.00 μ_B proves that NaVF3 material demonstrates half-metallic characteristics. The primary contribution to the total magnetic moment comes from the V atom, with minimal contributions from the Na along with F atoms.

Table 2 *Band gaps, Total and Individual Magnetic Moments of $NaVF_3$*

Mode of calculation	Band gap (eV)	Total magnetization (μ_B)	Na (μ_B)	V (μ_B)	F (μ_B)
PBE	5.7436	3.0000	0.0224	2.1536	0.0281
PBEsol	5.9325	3.0000	0.0316	2.0890	0.0252
Other calculations	5.1[a], 3.72[b]				

[a]Theoretical (TB-mBJ) (Chenine et al., 2017); [b]Theoretical (PBE) (Chenine et al., 2017)

Figure 2 *Band Diagram of (a) Spin up and (b) Spin down State for PBE*

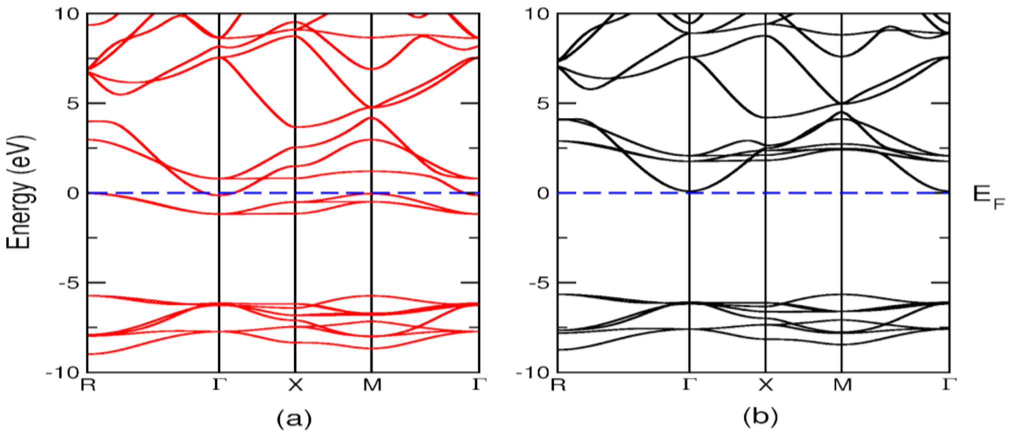

Figure 3 *Band Diagram of (a) Spin up and (b) Spin down State for PBEsol*

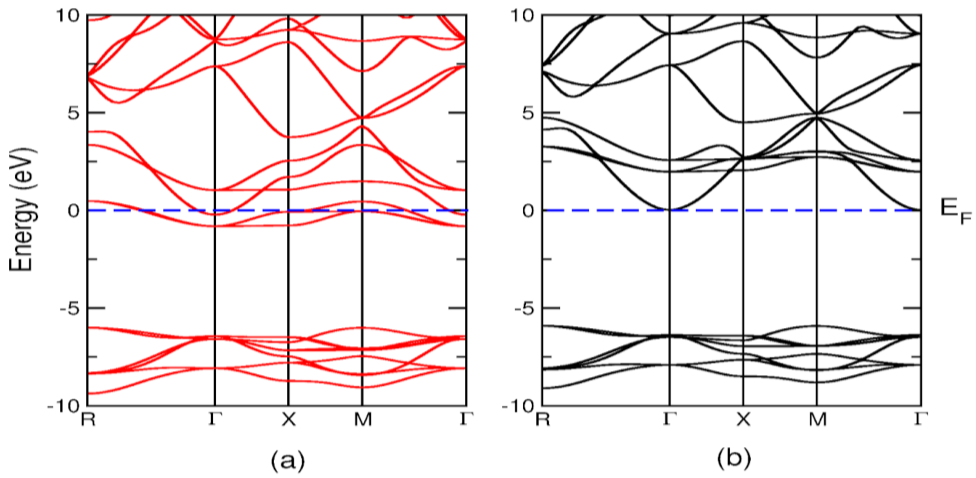

ISSN: 2976-1379 (Print)
ISSN: 2976-1387 (Online)

Figure 4 *Density of States of NaVF3 for PBE*

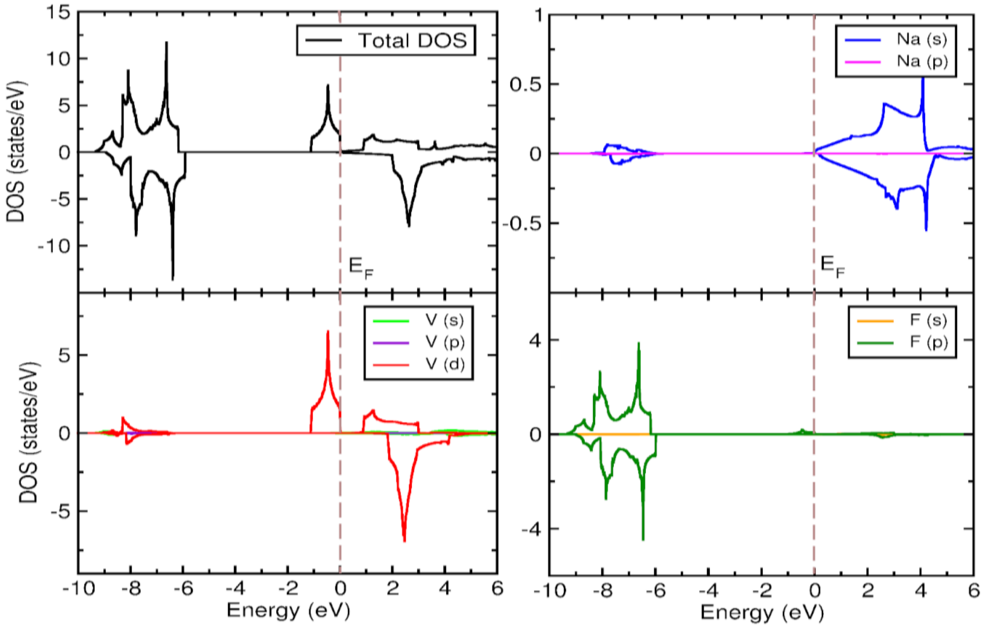

Figure 5 *Density of States of NaVF3 for PBEsol*

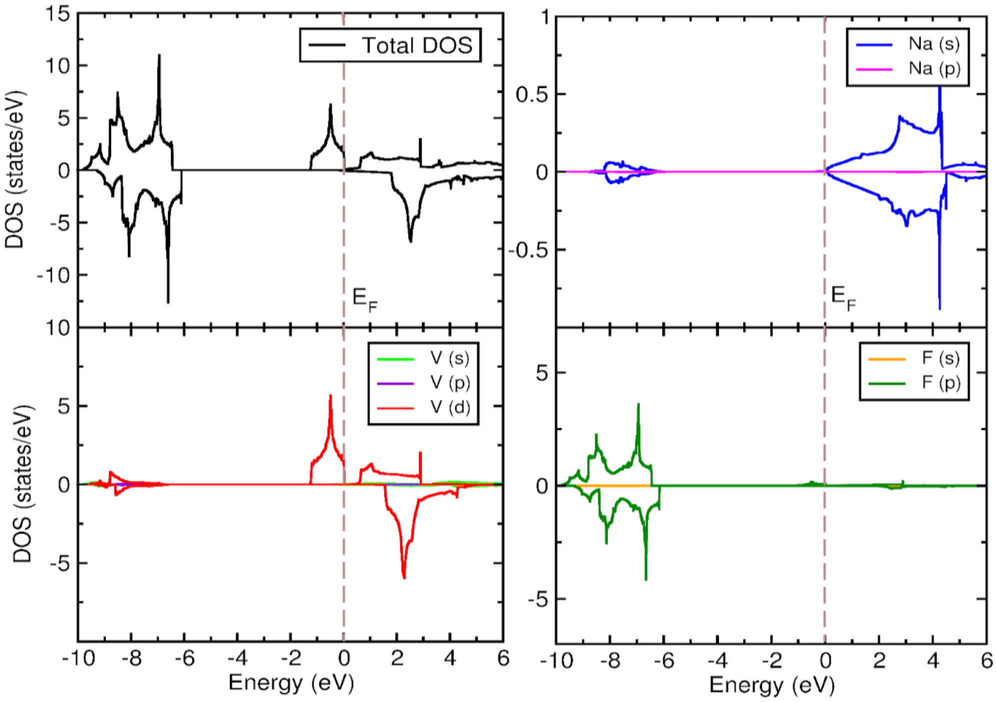

Mechanical Properties

To assure mechanical stability, the three independent elastic constants C_{11}, C_{12}, and C_{44} should satisfy the criteria proposed by Born (Born & Huang, 1956): $C_{11} - C_{12} > 0$; $C_{11} + 2C_{12} > 0$; $C_{44} > 0$. The calculated elastic constants are presented in Table 3, and it is evident that these elastic constants satisfy the criteria for mechanical stability. The elastic constants C_{11} and C_{12} indicate the response of the solid to uniaxial strain, while C_{44} describes the resistance to shape deformation. The significantly higher values of C_{11} and C_{12} compared to C_{44} suggest that the compound is less resistant to shear deformation than to uniaxial deformation. From the calculated elastic constants, various elastic properties including bulk modulus, shear modulus, Young's modulus and Poisson's ratio can be estimated using Voigt, Reuss and Hill estimations (Voigt, 1966; Hill, 1952; Reuss, 1929). The Voigt bulk modulus and Reuss bulk modulus of elasticity are equal in the cubic system (Dewit, 2008).

$$B = \frac{1}{3}(C_{11} + 2C_{12})$$

$$G = \frac{G_v + G_R}{2}$$

Where, $G_v = \frac{1}{5}(C_{11} - C_{12} + 3C_{44})$ and $G_R = \frac{5C_{44}(C_{11} - C_{12})}{4c_{44} + 3(C_{11} - C_{12})}$

$$E = \frac{9BG}{3B+G}$$

$$v = \frac{3B-2G}{2(3B+G)}$$

$$A = \frac{2C_{44}}{C_{11} - C_{12}}$$

Table 3 *The calculated elastic constants (C_{11}, C_{12} and C_{44}), bulk modulus (B), Young's modulus (E), shear modulus (G), Poisson's ratio (v), and Pugh's ratio (B/G)*

Mode of calculation	C_{11} (GPa)	C_{12} (GPa)	C_{44} (GPa)	B (GPa)	E (GPa)	G (GPa)	v	B/G
PBE	151.61	29.65	8.77	70.30	57.80	21.49	0.31	3.27
PBEsol	170.48	32.26	7.01	78.33	57.76	21.40	0.27	3.66
Other calculations	215.35[a]	36.90[a]	9.33[a]	96.38[a]	76.39[a]	27.92[a]	0.37[a]	3.45[a]

[a]Theoretical (Chenine, 2017)

According to Pugh's formula (Pugh, 1954), the Pugh ratio (B/G) is crucial in determining the brittleness of a material. B/G higher than 1.75 indicates ductility,

 ISSN: 2976-1379 (Print)
ISSN: 2976-1387 (Online)

while lower than 1.75 suggests brittleness. For $NaVF_3$, the values of B/G were obtained as 3.27 and 3.66 with PBE and PBEsol, respectively. Thus, the ductile nature of $NaVF_3$ can be confirmed. Poisson's ratio (v) can also be used to estimate the ductile or brittle nature of materials. Generally, if the value of Poisson's ratio (v) is less than 0.26, the material is considered brittle, whereas a value greater than 0.26 indicates ductility (Frantsevich, 1982). According to our calculations, the Poisson's ratio of $NaVF_3$ is 0.34 using the PBE functional and 0.35 using the PBEsol functionals. Therefore, it can be concluded that $NaVF_3$ is ductile in nature. Elastic anisotropy refers to the property of a material that leads to different elastic behavior along different crystallographic directions. It influences a range of physical phenomena, including phase transformations, anomalous phonon modes, anisotropic plastic deformation, precipitation processes, dislocation dynamics, mechanical yield strength, elastic instability, crack propagation, and internal friction (Nasir et al., 2017). A perfectly uniform material, called isotropic, would have the same value of modulus of elasticity in all directions. A perfectly isotropic material has anisotropy value of 1, while any value greater or less than 1 represents the degree of anisotropy (Zener, 1948). For $NaVF_3$, the anisotropy factors were found to be 0.14 and 0.10 for PBE and PBEsol respectively, indicating the anisotropic character of the studied material.

Furthermore, elastic constants allow the calculation of longitudinal and transverse sound velocities in a material using Navier's equations, which can then be used to estimate the average sound velocity (Anderson, 1963).

$$v_l = \left(\frac{3B+4G}{3\rho}\right)^{1/2}, \; v_t = \left(\frac{G}{\rho}\right)^{1/2}$$

$$v_m = \left[\frac{1}{3}\left(\frac{2}{v_t^3} + \frac{1}{v_l^3}\right)\right]^{-1/3}$$

Moreover, the Debye temperature ($\boldsymbol{\theta_D}$) can be estimated by using the average sound velocity as follows:

$$\theta_D = \frac{h}{k_B}\left[\frac{3n}{4\pi}\left(\frac{N_A\rho}{M}\right)\right]^{1/3} v_m$$

Table 4 summarizes all the calculated values of longitudinal, transverse, and average sound velocities and Debye temperature. It can be seen from the table that the material exhibits a high Debye temperature, which suggests that it may possess significant thermal conductivity. The calculated Debye temperature is in close agreement with the previously reported result (Chenine, 2017).

To further analyze the anisotropic characteristics of the material, 3D plots of Young's modulus, shear modulus, and Poisson's ratio were generated using the ELATE program (Gaillac et al., 2016), as illustrated in Figure 6. The non-spherical shapes of all three plots clearly confirm the anisotropic nature of the material, consistent with the anisotropy factor reported in Table 4.

Table 4 *Calculated longitudinal velocity of sound (v_l), transverse velocity of sound (v_t), average velocity (v_m), Debye temperature (θ_D), and anisotropy factor (A)*

Mode of calculation	v_l (m/s)	v_t (m/s)	v_m (m/s)	θ_D (K)	A
PBE	5648.21	2632.24	2963.98	328.25	0.14
PBEsol	5730.51	2564.19	2892.70	308.92	0.10

Figure 6 *3D visualizations of Young's modulus, shear modulus, and Poisson's ratio for $NaVF_3$*

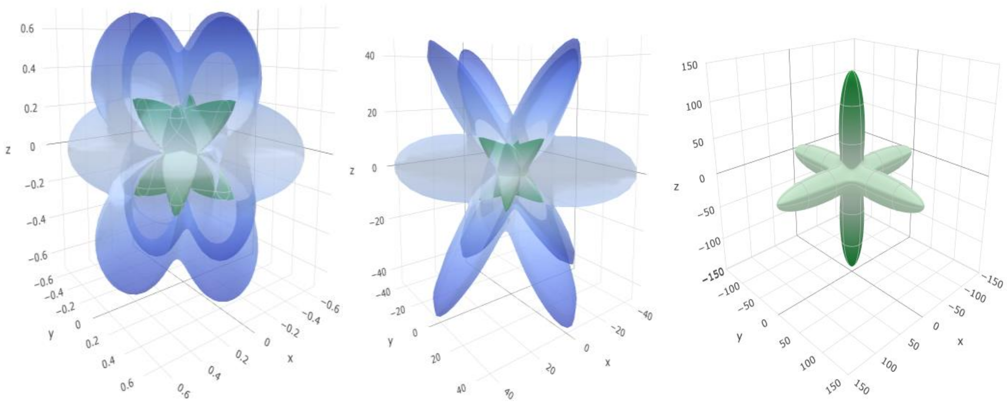

Conclusion

The structural, electronic, magnetic, and elastic properties of cubic $NaVF_3$ were computed using density functional theory. The study shows that $NaVF_3$ is mechanically stable, satisfying the Born criteria. The lattice parameters predicted by PBE and PBEsol functionals are in good agreement with the previously reported theoretical and experimental results. Band structures predict the half-metallic ferromagnetism with a wide band gap in the minority spin channel. The obtained values of band gaps are 5.74 eV and 5.93 eV for PBE and PBEsol, respectively. The integral value of the total magnetic moment further confirms the half-metallic nature of $NaVF_3$. The elastic constants, including bulk modulus, Young's modulus, shear modulus, Poisson's ratio, velocity of sound, and Debye temperature, are also reported in this work. The elastic calculations show that $NaVF_3$ is anisotropic and ductile.

ISSN: 2976-1379 (Print)
ISSN: 2976-1387 (Online)

Conflict of Interest

The authors declare no conflict of interest.

Authors Contribution

K K: conceptualization, methodology, formal analysis, and writing original draft.

U C: data validation, data visualization, and Writing—review and editing.

E T: software handling, formal analysis, and writing original draft

G C K: resources, supervision, data validation, data visualization, and writing—review and editing

References

Abdullah, N., Khan, U. A., Khan, S., Ahmed, S. J., Khan, N. U., Ullah, H., Naz, S., Farhat, L. B., Amami, M., Tirth, V., & Zaman, A. (2022). Structural, electronic and optical properties of Titanium based Fluoro-Perovskites MTIF3 (M = RB and CS) via Density Functional Theory Computation. *ACS Omega*, *7*(51), 47662-47670. https://doi.org/10.1021/acsomega.2c04631

Abdullah, N., Sajjad, M., Khan, U. A., Ullah, H., Alhodaib, A., Amami, M., Tirth, V., Zaman, A., & Shazia, N. (2022). Structural, electronic, magnetic and elastic properties of xenon-based fluoroperovskites XeMF3 (M = Ti, V, Zr, Nb) via DFT studies. *RSC Advances*, *12*(42), 27508-27516. https://doi.org/10.1039/d2ra05152d

Algahtani, A., Khan, N. U., Abdullah, N., Iqbal, J., Tirth, V., Abdullaev, S., Refat, M. S., Alsuhaibani, A. M., Henaish, A., Zaman, A., & Fetooh, H. (2023). Exploring the structural, opto-electronics and elastic properties of fluoro-perovskites KXF3 (X = Ir, Rh): A first-principles study. *Inorganic Chemistry Communications*, *158*, 111542. https://doi.org/10.1016/j.inoche.2023.111542

Anderson, O. L. (1963). A simplified method for calculating the debye temperature from elastic constants. *Journal of Physics and Chemistry of Solids*, *24*(7), 909-917. https://doi.org/10.1016/0022-3697(63)90067-2

Attema, J., Chioncel, L., Fang, C., De Wijs, G., & De Groot, R. (2005). Half-Metals: Challenges in Spintronics and routes toward solutions. In *Lecture notes in physics* (pp. 199-216). https://doi.org/10.1007/11417255_13

Babu, K. E., Neeraja, K., Deenabandhu, D., Ratna, A. M. V., Kumar, V. V., Kumari, K. B., Taddesse, P., Aregai, G. T., Mehar, M., Babu, B. V., Samatha, K., & Veeraiah, V. (2020). First-principles study of structural, elastic, electronic and optical properties of cubic perovskite LiMgF3 for novel applications.

Journal of Physics Conference Series, *1495*(1), 012010. https://doi.org/10.1088/1742-6596/1495/1/012010

Born, M., & Huang, K. (1956). *Dynamical theory of crystal lattices*.

Brittman, S., Adhyaksa, G. W. P., & Garnett, E. C. (2015). The expanding world of hybrid perovskites: materials properties and emerging applications. *MRS Communications*, *5*(1), 7-26. https://doi.org/10.1557/mrc.2015.6

Chenine, D., Aziz, Z., Benstaali, W., Bouadjemi, B., Youb, O., Lantri, T., Abbar, B., & Bentata, S. (2017). Theoretical investigation of Half-Metallic ferromagnetism in Sodium-Based fluoro-perovskite NAXF3 (X = V, Co). *Journal of Superconductivity and Novel Magnetism*, *31*(1), 285-295. https://doi.org/10.1007/s10948-017-4204-4

deWit, R. (2008). Elastic constants and thermal expansion averages of a nontextured polycrystal. *Journal of Mechanics of Materials and Structures*, *3*(2), 195–212. https://doi.org/10.2140/jomms.2008.3.195

Erum, N., & Iqbal, M. A. (2017). Physical properties of fluorine based perovskites for vacuum-ultraviolet-transparent lens materials. *Chinese Journal of Physics*, *55*(3), 893-903. https://doi.org/10.1016/j.cjph.2016.09.011

Frantsevich, I. N. (1982). Elastic constants and elastic moduli of metals and insulators. *Reference book*. https://ci.nii.ac.jp/naid/10004038718/

Gaillac, R., Pullumbi, P., & Coudert, F. (2016). ELATE: an open-source online application for analysis and visualization of elastic tensors. *Journal of Physics Condensed Matter*, *28*(27), 275201. https://doi.org/10.1088/0953-8984/28/27/275201

Giannozzi, P., Andreussi, O., Brumme, T., Bunau, O., Nardelli, M. B., Calandra, M., Car, R., Cavazzoni, C., Ceresoli, D., Cococcioni, M., Colonna, N., Carnimeo, I., Corso, A. D., De Gironcoli, S., Delugas, P., DiStasio, R. A., Ferretti, A., Floris, A., Fratesi, G., . . . Baroni, S. (2017). Advanced capabilities for materials modelling with Quantum ESPRESSO. *Journal of Physics Condensed Matter*, *29*(46), 465901. https://doi.org/10.1088/1361-648x/aa8f79

Giannozzi, P., Baroni, S., Bonini, N., Calandra, M., Car, R., Cavazzoni, C., Ceresoli, D., Chiarotti, G. L., Cococcioni, M., Dabo, I., Corso, A. D., De Gironcoli, S., Fabris, S., Fratesi, G., Gebauer, R., Gerstmann, U., Gougoussis, C., Kokalj, A., Lazzeri, M., . . . Wentzcovitch, R. M. (2009). QUANTUM ESPRESSO: a modular and open-source software project for quantum simulations of materials. *Journal of Physics Condensed Matter*, *21*(39), 395502. https://doi.org/10.1088/0953-8984/21/39/395502

Gillani, S. S. A., Fatima, N., Shakil, M., Kiran, R., Tahir, M. B., Jawad, A., & Ahmad, R. (2021). Ultra-wide bandgap semiconductor behavior of NaCaF3 fluoro-perovskite

ISSN: 2976-1379 (Print)
ISSN: 2976-1387 (Online)

with external static isotropic pressure and its impact on optical properties: First-principles computation. *Research Square (Research Square)*. https://doi.org/10.21203/rs.3.rs-336152/v1

Hamlat, M., Boudia, K., Amara, K., Khelfaoui, F., & Marbouh, N. (2020). Half-metallic stability of the cubic Perovskite KMgO3. *Computational Condensed Matter*, *23*, e00456. https://doi.org/10.1016/j.cocom.2020.e00456

Hashmi, M. R. U. R., Zafar, M., Shakil, M., Sattar, A., Ahmed, S., & Ahmad, S. A. (2016). First-principles calculation of the structural, electronic, and magnetic properties of cubic perovskite Rb X F 3 (X = Mn, V, Co, Fe). *Chinese Physics B*, *25*(11), 117401. https://doi.org/10.1088/1674-1056/25/11/117401

Hill, R. (1952). The elastic behaviour of a crystalline aggregate. *Proceedings of the Physical Society Section A*, *65*(5), 349–354. https://doi.org/10.1088/0370-1298/65/5/307

Hohenberg, P., & Kohn, W. (1964). Inhomogeneous electron gas. *Physical Review*, *136*(3B), B864–B871. https://doi.org/10.1103/physrev.136.b864

Jain, A., Ong, S. P., Hautier, G., Chen, W., Richards, W. D., Dacek, S., Cholia, S., Gunter, D., Skinner, D., Ceder, G., & Persson, K. A. (2013). Commentary: The Materials Project: A materials genome approach to accelerating materials innovation. *APL Materials*, *1*(1). https://doi.org/10.1063/1.4812323

Khattak, S. A., Abohashrh, M., Ahmad, I., Husain, M., Ullah, I., Zulfiqar, S., Rooh, G., Rahman, N., Khan, G., Khan, T., Khan, M. S., Shah, S. K., & Tirth, V. (2023). Investigation of structural, mechanical, optoelectronic, and thermoelectric properties of BAXF3 (X = Co, IR) Fluoro-Perovskites: Promising materials for optoelectronic and thermoelectric applications. *ACS Omega*, *8*(6), 5274-5284. https://doi.org/10.1021/acsomega.2c05845

Kohn, W., & Sham, L. J. (1965). Self-Consistent equations including exchange and correlation effects. *Physical Review*, *140*(4A), A1133-A1138. https://doi.org/10.1103/physrev.140.a1133

Meziani, A., Heciri, D., & Belkhir, H. (2011). Structural, electronic, elastic and optical properties of fluoro-perovskite KZnF3. *Physica B Condensed Matter*, *406*(19), 3646-3652. https://doi.org/10.1016/j.physb.2011.06.063

Monkhorst, H. J., & Pack, J. D. (1976). Special points for Brillouin-zone integrations. *Physical Review. B, Solid State*, *13*(12), 5188-5192. https://doi.org/10.1103/physrevb.13.5188

Motornyi, O., Raynaud, M., Corso, A. D., & Vast, N. (2018). Simulation of electron energy loss spectra with the turboEELS and thermo_pw codes. *Journal of Physics Conference Series*, *1136*, 012008. https://doi.org/10.1088/1742-6596/1136/1/012008

Mubarak, A., & Al-Omari, S. (2015). First-principles calculations of two cubic fluoropervskite compounds: RbFeF3 and RbNiF3. *Journal of Magnetism and Magnetic Materials*, *382*, 211-218. https://doi.org/10.1016/j.jmmm.2015.01.073

Murnaghan, F. D. (1944). The Compressibility of Media under Extreme Pressures. *Proceedings of the National Academy of Sciences*, *30*(9), 244-247. https://doi.org/10.1073/pnas.30.9.244

Nasir, M. T., Hadi, M. A., Rayhan, M. A., Ali, M. A., Hossain, M. M., Roknuzzaman, M., Naqib, S. H., Islam, A. K. M. A., Uddin, M. M., & Ostrikov, K. (2017). First-Principles Study of Superconducting ScRhP and ScIrP pnictides. *Physica Status Solidi (B)*, *254*(11). https://doi.org/10.1002/pssb.201700336

Neupane, K., & Thapa, R. K. (2017). Study of Structural and Electronic Properties of Fluoride Perovskite KCaF3 using FP-LAPW Method. *Himalayan Physics*, 100-103. https://doi.org/10.3126/hj.v6i0.18370

Perdew, J. P., Burke, K., & Ernzerhof, M. (1996). Generalized gradient approximation made simple. *Physical Review Letters*, *77*(18), 3865-3868. https://doi.org/10.1103/physrevlett.77.3865

Perdew, J. P., Chevary, J. A., Vosko, S. H., Jackson, K. A., Pederson, M. R., Singh, D. J., & Fiolhais, C. (1992). Atoms, molecules, solids, and surfaces: Applications of the generalized gradient approximation for exchange and correlation. *Physical Review. B, Condensed Matter*, *46*(11), 6671-6687. https://doi.org/10.1103/physrevb.46.6671

Perdew, J. P., Ruzsinszky, A., Csonka, G. I., Vydrov, O. A., Scuseria, G. E., Constantin, L. A., Zhou, X., & Burke, K. (2008). Restoring the Density-Gradient expansion for exchange in solids and surfaces. *Physical Review Letters*, *100*(13). https://doi.org/10.1103/physrevlett.100.136406

Pilania, G., & Sharma, V. (2013). First principles investigations of structural, electronic, elastic, and dielectric properties of KMgF3. *Journal of Materials Science*, *48*(21), 7635–7641. https://doi.org/10.1007/s10853-013-7581-5

Pugh, S. (1954). XCII. Relations between the elastic moduli and the plastic properties of polycrystalline pure metals. *The London Edinburgh and Dublin Philosophical Magazine and Journal of Science*, *45*(367), 823–843. https://doi.org/10.1080/14786440808520496

Rahman, M. A., Babu, M. M. H., Karimunnesa, S., & Kholil, M. I. (2021). Properties of RbHgF3 fluoro-perovskite under growing hydrostatic pressure from first-principles calculations. *AIP Advances*, *11*(11). https://doi.org/10.1063/5.0068050

Rahman, N., Husain, M., Sohail, M., Khan, R., Zaman, T., Neffati, R., Murtaza, G., Khan, A., Khan, A. A., & Iqbal, Z. (2023). Exploring the structural, optoelectronic, elastic, and thermoelectric properties of cubic ternary fluoro-perovskites sodium based NaMF3 (M = Si and Ge) compounds for heterojunction solar cells applications. *Physica Scripta*, *98*(6), 065929. https://doi.org/10.1088/1402-4896/accfc5

Rashid, M. (2019). Study of vanadium difluoride AVF3 (A = NA, K, RB) for optoelectronic and thermoelectric device applications via AB initio calculations. *Journal of Superconductivity and Novel Magnetism*, *33*(4), 1167-1175. https://doi.org/10.1007/s10948-019-05317-z

ISSN: 2976-1379 (Print)
ISSN: 2976-1387 (Online)

Ray, R. B., Rai, R. K., Yadav, D. K., & Kaphle, G. C. (2024). Exploring Femnval Heusler Alloy: Physical, mechanical, and magnetic properties. *Journal of Lumbini Engineering College*, *6*(1), 93-104. https://doi.org/10.3126/lecj.v6i1.66288

Rehman, J. U., Usman, M., Tahir, M. B., Hussain, A., Rehman, M. A., Sagir, M., Alrobei, H., Ullah, S., & Assiri, M. A. (2021). First-principles calculations to investigate ultra-wide bandgap semiconductor behavior of NaMgF3 fluoro-perovskite with external static isotropic pressure and its impact on optical properties. *Optik*, *252*, 168532. https://doi.org/10.1016/j.ijleo.2021.168532

Reuss, A. (1929). Berechnung der Fließgrenze von Mischkristallen auf Grund der Plastizitätsbedingung für Einkristalle . *ZAMM - Journal of Applied Mathematics and Mechanics / Zeitschrift Für Angewandte Mathematik Und Mechanik*, *9*(1), 49–58. https://doi.org/10.1002/zamm.19290090104

Sandeep, N., Rai, D., Shankar, A., Ghimire, M., Khenata, R., Omran, S. B., Syrotyuk, S., & Thapa, R. (2017). Investigation of the structural, electronic and optical properties of the cubic RbMF 3 perovskites (M = Be, Mg, Ca, Sr and Ba) using modified Becke-Johnson exchange potential. *Materials Chemistry and Physics*, *192*, 282-290. https://doi.org/10.1016/j.matchemphys.2017.02.005

Shafer, M. (1969). The synthesis and characterization of vanadium difluoride, NaVF3, KVF3, and RbVF3. *Materials Research Bulletin*, *4*(12), 905-912. https://doi.org/10.1016/0025-5408(69)90047-6

Shahzad, M. K., Hussain, S., Riaz, M., Sattar, H., Ashraf, G. A., Azeem, W., Ali, S. M., & Alam, M. (2024). Investigation of ultra wide bandgap Flouro-perovskite materials RBeF3 (R K and Li) for smart window applications: A DFT study. *Heliyon*, *10*(7), e29143. https://doi.org/10.1016/j.heliyon.2024.e29143

Voigt, W. (1966). *Lehrbuch der Kristallphysik*. https://doi.org/10.1007/978-3-663-15884-4

Zener, C. (1948). *Elasticity and anelasticity of metals*.